

RESEARCH

Open Access



Temperature dependence of thermophysical properties of carbon/polyamide410 composite

Kasahun Niguse Asfew^{1,2*}, Jan Ivens¹ and David Moens³

Abstract

In this study, the temperature dependence of the carbon/polyamide 410 composite's heat capacity, thermal expansion, density, and thermal conductivity was investigated. The results demonstrated that the specific heat capacity of the C/PA410 composite increases with temperature, with major transitions observed at the glass transition (T_g) and melting (T_m) temperatures. Due to the presence of fibers, the CTE values in the fiber direction of C/PA410 specimens were one order of magnitude smaller than in the transverse direction. The density measurements reveal that as temperature rises, volume increases, causing density to decrease. The heat diffusivity of the C/PA410 composite was measured using the laser flash technique, which was then used to calculate thermal conductivity. The results show that the average thermal conductivity in the fiber direction increases linearly with temperature, while in the transverse direction it increases linearly with temperature up to 50 °C and then becomes constant between 50 °C and 100 °C.

Keywords: Temperature dependence, Carbon/polyamide composites, Specific heat capacity, Coefficient of thermal expansion, Thermal conductivity

Introduction

In the production of thermoplastic composite products, the material must be processed at high temperatures, which affects its thermophysical properties. Accurate thermal simulations require knowledge of temperature-dependent thermophysical properties. Consequently, it is becoming increasingly important to investigate the behavior of thermoplastic composites at elevated temperatures. The effect of temperature on thermal diffusivity, thermal conductivity, heat capacity, coefficient of thermal expansion (CTE), and density of isotropic or anisotropic materials has been the subject of research by several scientists. The studies [1–4] used the laser flash method, transient plane source (TPS) [5], and modulated DSC [6] to determine the thermal diffusivity, derived heat capacity, and thermal conductivity of isotropic metals and fiber-reinforced polymer composites (FRPC).

The effects of the finite width of the laser flash pulse, heat loss, and specimen thickness in thermal diffusivity measurement [7] and the influence of the stacking sequence of composite specimens and frequency of the source on thermal wave distribution [8] in the laser flash method have been studied. In the laser flash method, a program was used to analyze and calculate thermal diffusivity values from images acquired using an IR camera [9]. The temperature dependence of specific heat capacity, thermal diffusivity, and thermal conductivity of different composite materials has been studied by several researchers [3]. The thermal conductivity of semi-crystalline and four amorphous polymers was determined starting at room temperature and [10] going up to temperatures above the polymer melting point (T_m) for semi-crystalline polymers or above the glass transition temperature (T_g) for amorphous polymers, and the peak thermal conductivity values are observed around T_g for amorphous and around T_m for semi-crystalline polymers. [11] presented a three-dimensional thermal diffusivity method using lock-in thermography for isotropic and anisotropic materials.

*Correspondence: Kasahunniguse.asfew@kuleuven.be

¹ Department of Materials Engineering, KU Leuven Campus De Nayer, J. De Nayerlaan 5, 2860 Sint-Katelijne-Waver, Belgium
Full list of author information is available at the end of the article

The coefficient of thermal expansion (CTE) of several FRPCs was studied at a wide range of temperatures, and the CTE was significantly affected by temperature and fiber direction [12, 13]. The temperature dependence of carbon/epoxy was determined, and both the in-plane and through-thickness thermal conductivities increased linearly with temperature [14]. Even though numerous researchers used various methods to assess how temperature affected the thermophysical properties of fiber-reinforced polymer composites, there hasn't been a comprehensive examination of C/PA410 in the literature. In this study, the effects of temperature on the heat capacity, thermal expansion, density, and thermal conductivity of a carbon/polyamide410 composite were investigated.

Material and methods

In this study, the material used for specimen preparation and testing is unidirectional C/PA410 tape with a 24% fiber content supplied by Sioen Industries.

Heat capacity of C/PA410 composite as a function of temperature

In this experiment, DSC thermograms were recorded with a DSC Q2000 V24.11 Build 124 (TA Instruments). Standard specimens of UD C/PA410 composite tapes with approximately 8–10 mg of mass were used. Liquid nitrogen was used as a purge gas at a flow rate of 50 mL/min. The specimens were equilibrated at -50 °C, and data was collected over a temperature range of -50 to 300 °C at a heating and cooling rate of 3.00 °C/min. There was an isothermal dwell of five minutes between each step.

CTE (coefficient of thermal expansion) of C/PA410 composite as a function of temperature

Thermal energy is responsible for atomic or molecular vibrations about a mean position in any material. As the temperature of the materials is increased, the amplitude of thermal energy-induced vibrations increases, and interatomic or intermolecular spacing increases, i.e., an expansion of the body occurs. In this work, thermomechanical measurements are performed on a C/PA410 composite specimen using a TA Instruments Q400 thermomechanical analyzer in expansion mode. The

procedure used in this study is presented in Table 1. The initial heating and cooling cycle outlined in the procedure for longitudinal CTE measurement is employed to relieve residual stresses accumulated during specimen preparation.

Density of C/PA410 composite as a function of temperature

From the values of volumetric expansion at different temperatures and the density at room temperature (20 °C), it is possible to determine how density varies with temperature. In this study, the Multipycnometer from Quantachrome Instruments was used to measure the density of 6 g C/PA410 composite specimens.

Thermal diffusivity and thermal conductivity of C/PA410 composite as a function of temperature

A diode laser source (MDL-N-808/7-10 W) was used to produce a thermal contrast on the specimen's surface to assess the thermal diffusivity of the C/PA410 specimen. The main laser source characteristics are shown in Table 2. A cylindrical lens expanded the laser beam to a vertical line (2 mm*6 mm), reflected it in the mirror, and focused on the specimen surface using a convex lens (f200), as shown in Fig. 1. The laser was directed to the surface of the specimen for two seconds during each run of the experiment, whereby the illuminated strip heated up and the heat began to disperse out of the lit zone. The laser source is then be blocked, allowing the heat to diffuse. An IR camera (CEDIP JADE UC J330R) set perpendicular to the specimen surface at 10 cm was used to record at a sampling frequency of 50 Hz. The main IR camera characteristics are summarized in Table 3. For each run of the experiment, the camera record the IR

Table 2 The main laser source characteristics

| Characteristics | Unit | Value |
|----------------------------------|------|---------|
| Wavelength | nm | 808 ± 3 |
| Output Power | mW | > 7000 |
| Warm Up Time | Min | 5 |
| Beam Diameter at The Aperture | mm | 5–8 |
| Pointing Stability After Warm Up | mrad | < 0.05 |

Table 1 TMA measurement procedure

| | CTE (Longitudinal) | CTE(Transverse) |
|---|--------------------------------------|-------------------------------------|
| 1 | Ramped heating (10 °C/min) to 200 °C | Cooling to -30 °C |
| 2 | Cooling (10 °C/min) up to -30 °C | Ramped heating (3 °C/min) to 200 °C |
| 3 | Ramped heating (3 °C/min) to 200 °C | Cooling (3 °C/min) up to 20 °C |
| 4 | Cooling (5 °C/min) up to 20 °C | |

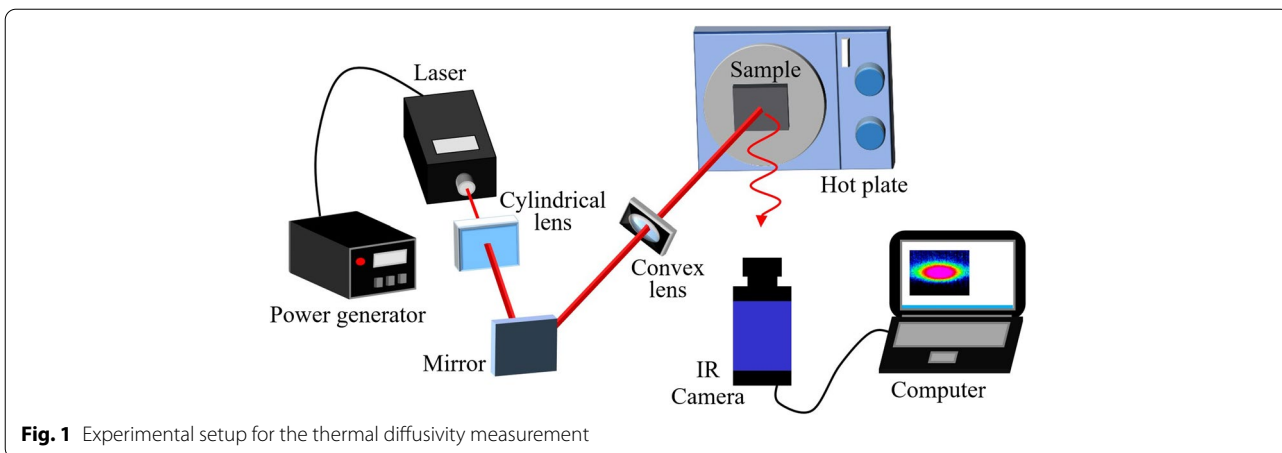


Table 3 The main IR camera characteristics

| Characteristics | Unit | Value |
|---------------------|--------|----------------------------|
| Resolution | Pixels | 320 (H) × 240 (V) |
| Sensor material | | Uncooled microbolometer |
| Spectral response | μm | 8–12 |
| Thermal sensitivity | mK | 80 @ F/0.8 @ 30 °C typical |
| Frame rate | Hz | 50 or 60 |

radiation emitted by the specimen for 15 s (2 s before the heating started, 2 s while heating, and 11 s during cooling). The amount of IR radiation observed is related to the change in temperature.

The test was performed on four identical specimens (30 mm*30 mm*1.5 mm) at four distinct temperatures: room temperature (25 °C), 50 °C, 85 °C, and 100 °C. At each temperature, two experiments were carried out, with the fibers aligned horizontally and vertically to quantify heat diffusion along with the fiber and perpendicular to it.

The temperature of the specimen was measured using a thermometer (thin-film standard PT1000 element,

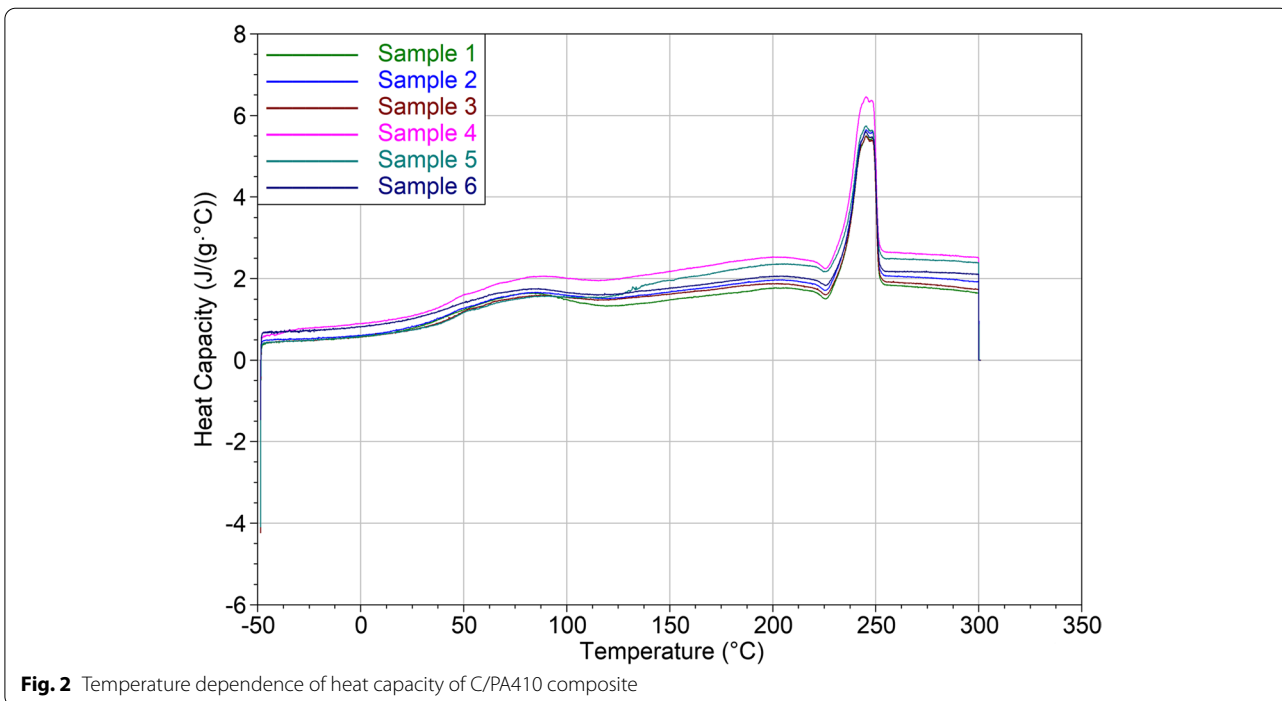


Table 4 Average specific capacity of C/PA410 composite in the linear section between transition temperatures

| | Average Specific Heat Capacity (J/g °C) | | |
|--------------|---|-------------------------------|---------------------|
| | Up to Tg (47.2 °C) | Tg (47.2 °C) to Tm (245.6 °C) | Above Tm (245.6 °C) |
| $\mu \pm SD$ | 0.74 ± 0.13 | 1.94 ± 0.2 | 2.44 ± 0.3 |

2*10 mm) affixed to the center part of the specimen as indicated in Fig. 1. A digital multimeter (34401A) from Keysight Technologies was used for data acquisition, and the LabVIEW (National Instruments Corporation, USA) environment was used for the temperature readings.

Results and discussions

Temperature dependance of heat capacity of C/PA410 composites

The result of the temperature dependence of heat capacity is shown in Fig. 2 and Table 4 presents it in three linear intervals between the transition temperatures.

In the beginning, the heat capacity of the specimen is increased slightly up to Tg, and the mean specific heat capacity was 0.74 J/g°C. Above Tg, the polymer structure is floppy and has sufficient free volume for various molecular motions to be able to absorb the added heat. The mean specific heat capacity between Tg and Tm then

becomes 1.96 J/g°C. The polymer’s crystalline regions then melt at Tm. At this stage, first, the polymer absorbs a certain amount of heat (the latent heat of melting); second, the polymer undergoes a change in heat capacity. Due to this, the mean specific heat capacity above Tm further increased to 2.44 J/g°C.

Temperature dependance of coefficient of thermal expansion (CTE) of C/PA410 composites

The temperature dependence of the longitudinal and transverse CTE of C/PA410 composite are presented in Figs. 3 and 4. An idealized TMA curve has a linear section below the transition (expansion below Tg) and a linear section above the transition (expansion above Tg). Tables 5 and 6 summarize the TMA measurements in the fiber and transverse directions, respectively. Similar to [12], this study demonstrated a significant difference in CTE based on fiber orientation.

In the direction of the fibers, the CTE is small because of the mechanical restraints imposed by the fibers. On the other hand, compared to the CTE in the fiber direction, more than an order of magnitude increase in CTE values is observed in the transverse direction. This effect is even more pronounced with increasing temperatures.

The higher CTE value of the polymer matrix mainly contributed to the higher expansion of the composite in the transverse direction. In addition, the rigid fibers

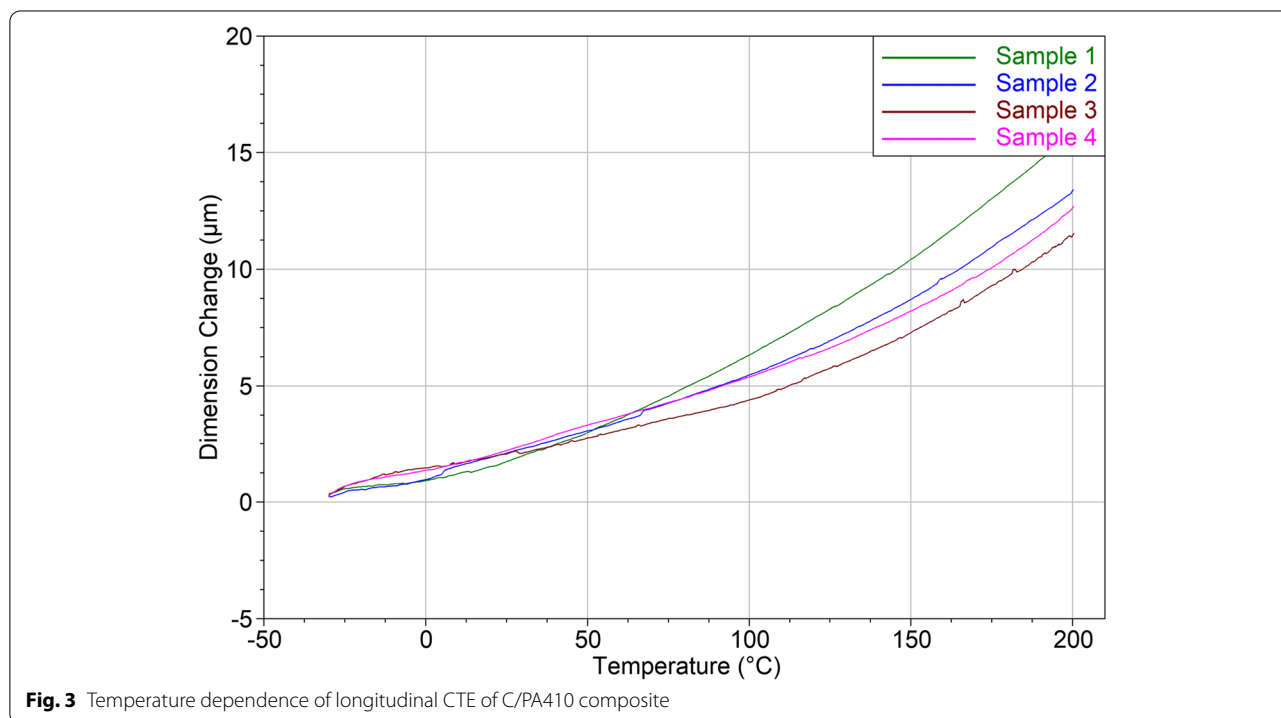
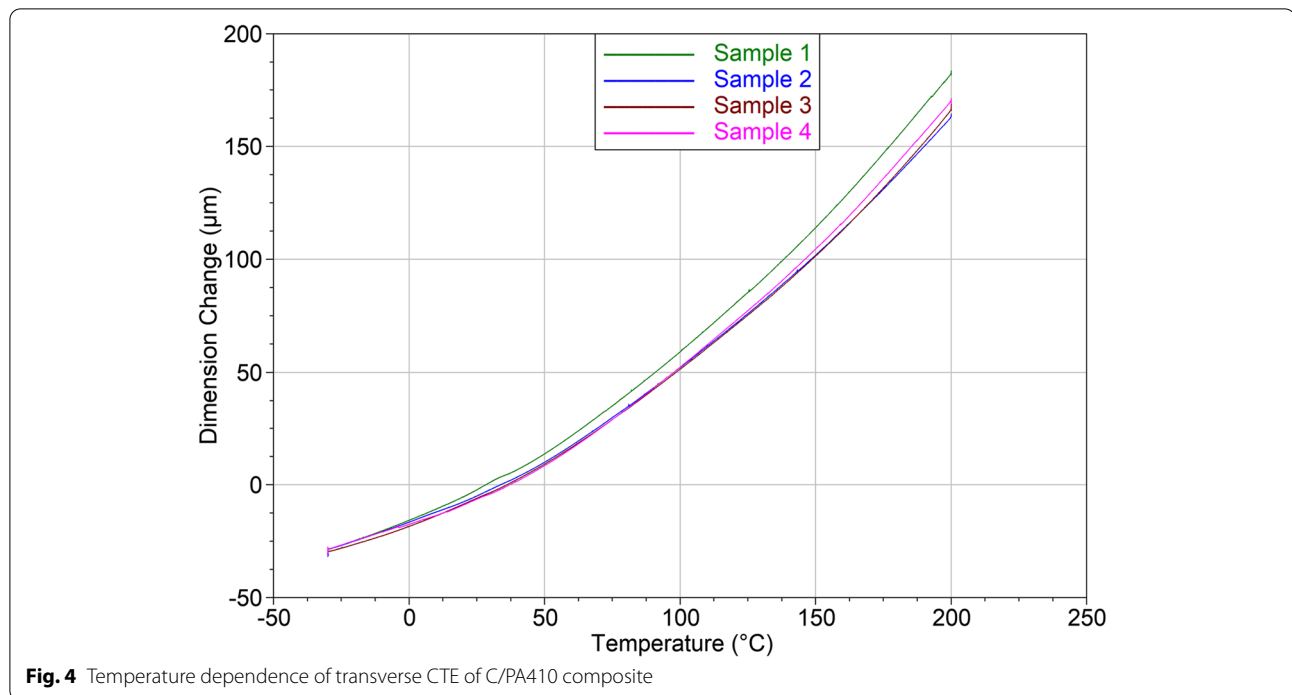


Fig. 3 Temperature dependence of longitudinal CTE of C/PA410 composite



restrict the matrix from expanding in the direction of the fibers, forcing the matrix to expand even more in the transverse direction. At T_g , a considerable increase in expansion rate and a change in the slope of the CTE curves are observed in both the fiber and transverse directions of the composite.

Temperature dependance of the density of C/PA410 composites

The measured density at room temperature (20 °C) was 1.22 g/cm³. The calculated evolution of the density of the C/PA410 composite over the temperature range of 20–200 °C (Fig. 5) shows that the density drops as temperature increases.

Temperature dependance of thermal diffusivity and thermal conductivity of C/PA410 composites

A program written for analysis is used to analyze the IR images of each specimen taken at different temperatures. Figure 6 provides a description of the analysis’s procedure. The temperature profiles over the width of the laser line were extracted and fitted using the Gaussian equation for each collected frame. From this, the FWHM progress with time is plotted. The thermal diffusivity is calculated using the slope of a linearly fitted cooling section of the $FWHM$ vs \sqrt{t} graph.

Since the $FWHM = 2.35 * \sqrt{2\alpha} * \sqrt{t}$, the slope of a linearly fitted cooling section of the $FWHM$ vs \sqrt{t} graph is used to calculate the thermal diffusivity (α) using Eq. (1):

$$\alpha = \frac{Slope}{2.35 * \sqrt{2}} \tag{1}$$

In Figs. 7 and 8, the temperature dependence of the rate of heat transfer (thermal diffusivity) along the fiber and transverse directions of the four C/PA410 specimens is illustrated, respectively.

As shown in Fig. 9, the average thermal diffusivity increased with temperature along the fiber direction and was distributed almost uniformly in the transverse direction.

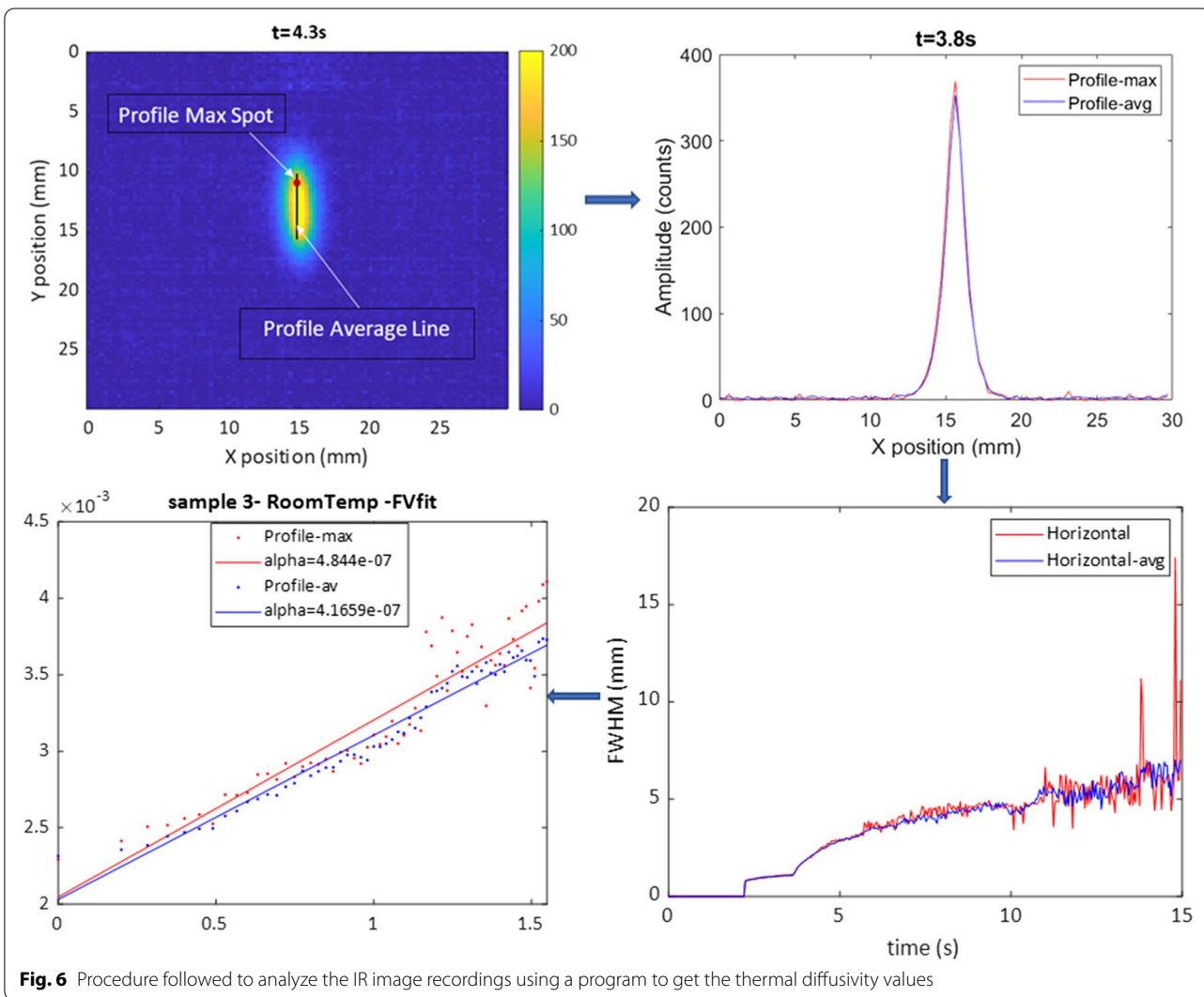
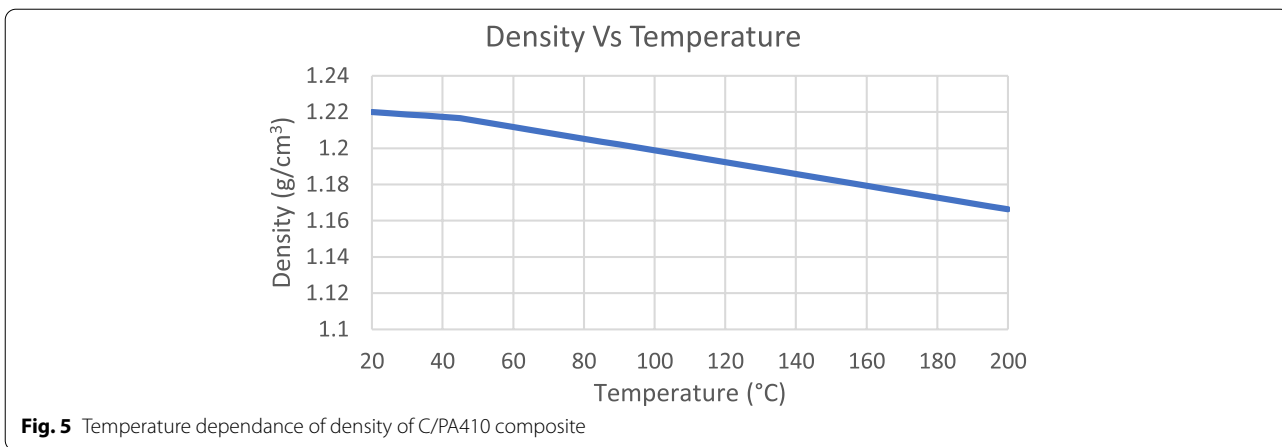
Thermal conductivity at each temperature is calculated from the average thermal diffusivity, specific heat

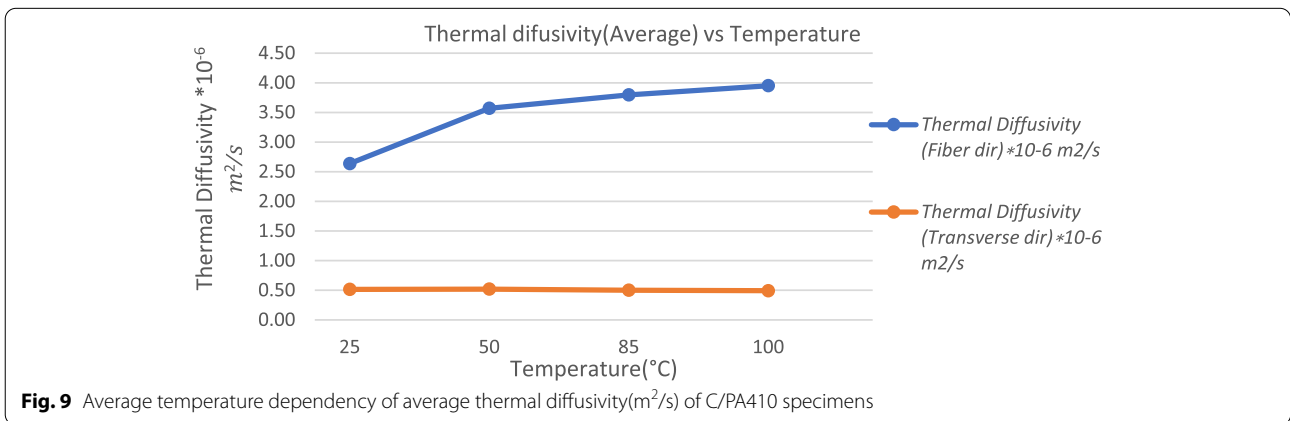
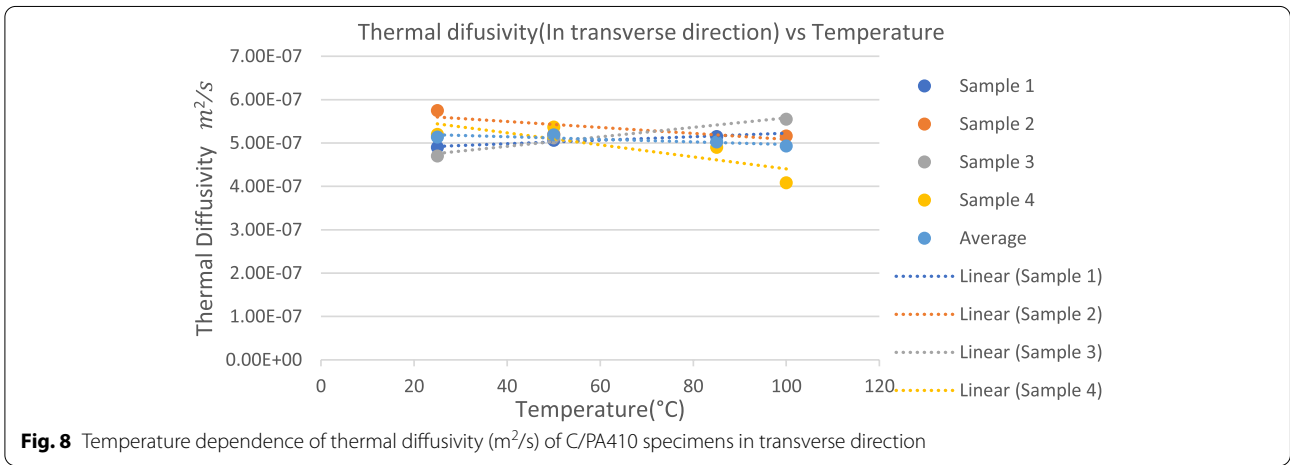
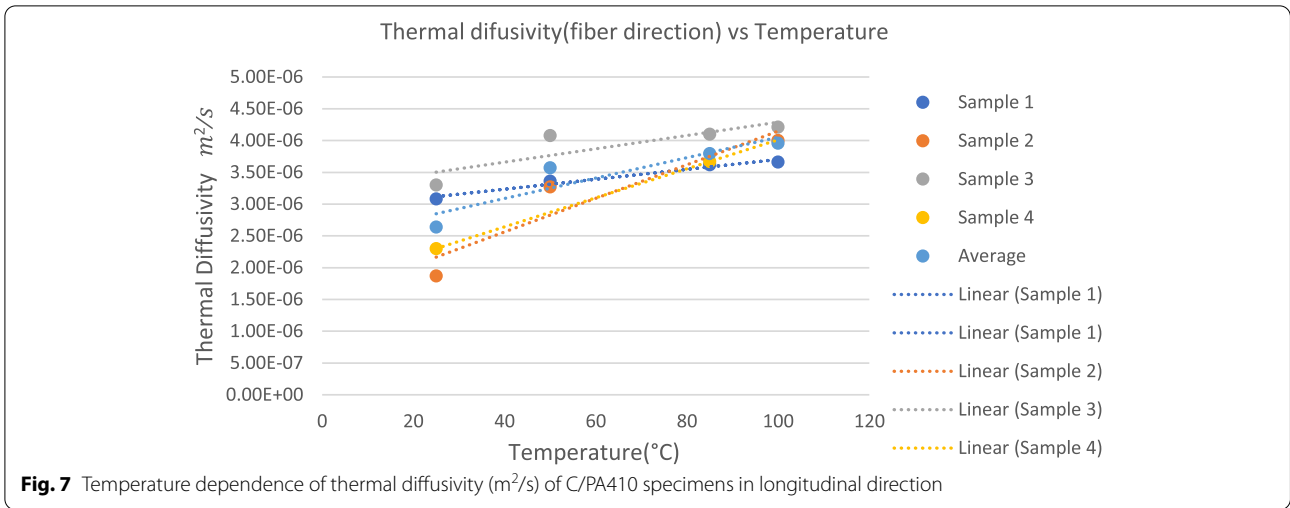
Table 5 Summary of the average CTE values along longitudinal direction

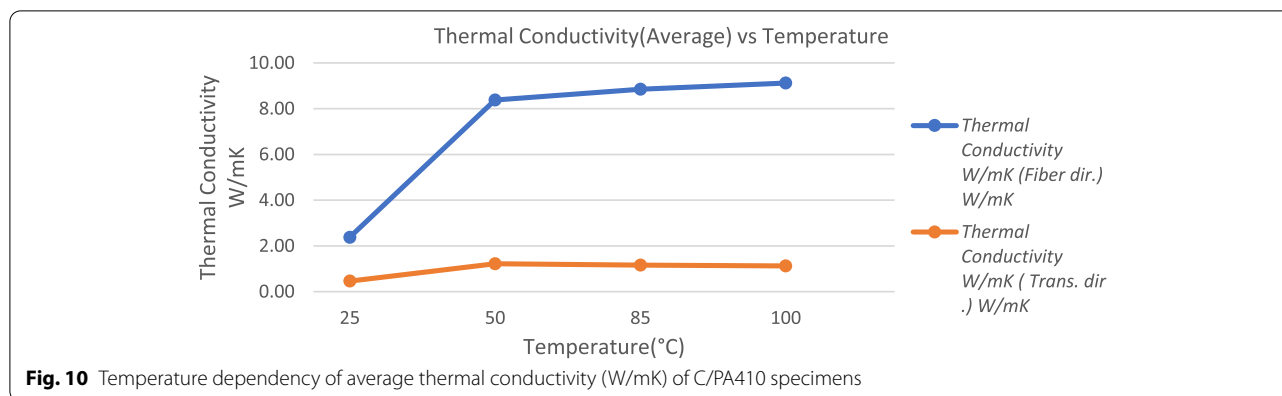
| | CTE below T_g (47.2 °C) $\mu m / (m^{\circ}C)$ | CTE above T_g (47.2 °C) $\mu m / (m^{\circ}C)$ |
|--------------------|---|---|
| CTE = $\mu \pm SD$ | 2.5 ± 0.4 | 6.75 ± 0.77 |

Table 6 Summary of the average CTE values along transverse direction

| | CTE below T_g (47.2 °C) $\mu m / (m^{\circ}C)$ | CTE above T_g (47.2 °C) $\mu m / (m^{\circ}C)$ |
|--------------------|---|---|
| CTE = $\mu \pm SD$ | 62.45 ± 6.2 | 159.4 ± 8.2 |







capacity, and density values at each temperature. The temperature-dependence trend of the thermal conductivity of C/PA410 is similar to the results obtained by [14] for the C/Epoxy composite. Figure 10 shows that the thermal conductivity of C/PA410 composites increases progressively with temperature along the fiber direction, with a small increase in the beginning and distributed almost uniformly later in the transverse direction for the temperature range between room temperature (25 °C) and 100 °C.

In nonmetals, increasing temperature increases the lattice vibration, giving higher phonon propagation. On the other hand, the density of the composite drops, and the heat capacity increases at higher temperatures. Due to the presence of highly conductive continuous carbon fibers, the thermal conductivity along the fiber direction increases with temperature, and heat conduction is dominated by lattice vibrations, but this effect is less potent along the transverse direction.

Conclusion

The thermophysical properties (heat capacity, thermal expansion, density, and thermal conductivity) of the C/PA410 composite have been examined in relation to temperature. The heat capacity of the specimens increased as the temperature rose, but the density decreased. The CTE of the specimens increased with temperature increment and at T_g , a significant increase in the rate of expansion was observed both in the fiber and transverse direction of the composite. Experimental results of the laser flash method showed that the thermal diffusivity and thermal conductivity of the specimens increase progressively with temperature along the fiber direction and are distributed almost uniformly in the transverse direction.

Abbreviations

C/PA410: Carbon/Polyamide 410; T_g : Glass Transition Temperatures; T_m : Melting Temperatures; CTE: Coefficient of Thermal Expansion; TPS: Transient Plane

Source; FRPC: Fiber-Reinforced Polymer Composites; FWHM: Full Width Half Maximum.

Acknowledgements

In this study, the thermal diffusivity measurement was carried out at the Laboratory of Acoustics and Thermal Physics (ATF) in the Department of Physics and Astronomy, KU Leuven, and we would like to express our gratitude to Professor Christ Glorieux for his tremendous assistance with the experiments.

Authors' contributions

Kasahun Niguse Asfew: Conceptualization, Design of the work, Investigation, interpretation of data, Validation, Writing (original draft), Visualization. Jan Ivens: Conceptualization, Design of the Work, Review & Editing, Supervision, Funding Acquisition David Moens: Conceptualization, Design of the Work, Review & Editing, Supervision, Funding Acquisition. The author(s) read and approved the final manuscript.

Funding

This research work was carried out in the frame of the HGPP project (International University Partnership Services for the Establishment of Postgraduate Programmes in Ethiopia) funded through GIZ GmbH and the International University Partnership for the Establishment of PhD Programmes in Ethiopia funded by the Ethiopian Ministry of Science and Higher Education.

Availability of data and materials

The raw or processed data required to reproduce these findings is available on request from the corresponding author.

Declarations

Ethics approval and consent to participate

Not applicable

Consent for publication

Not applicable

Competing interests

The authors declare that they have no known competing financial or non-financial interests or personal relationships that could have appeared to influence the work reported in this paper.

Author details

¹Department of Materials Engineering, KU Leuven Campus De Nayer, J. De Nayerlaan 5, 2860 Sint-Katelijne-Waver, Belgium. ²Department of Mechanical Engineering, Adama Science and Technology University, P.O. Box: 1888, Adama, Ethiopia. ³Department of Mechanical Engineering, KU Leuven Campus De Nayer, J. De Nayerlaan 5, 2860 Sint-Katelijne-Waver, Belgium.

Received: 28 August 2022 Accepted: 8 November 2022

Published online: 28 November 2022

References

1. C. Boué, D. Fournier, Infrared Thermography Measurement of the Thermal Parameters (Effusivity, Diffusivity and Conductivity) of Materials. *Quant Infrared Thermogr J* **6**, 175 (2009)
2. J.C. Krapez, L. Spagnolo, M. Frieß, H.P. Maier, Günter Neuer, Measurement of In-Plane Diffusivity in Non-Homogeneous Slabs by Applying Flash Thermography. *Int J Ther Sci* **43**, 967 (2004)
3. G. Spinelli, R. Guarini, R. Kotsilkova, T. Batakliiev, E. Ivanov, V. Romano, Experimental and Simulation Studies of Temperature Effect on Thermophysical Properties of Graphene-Based Polylactic Acid. *Materials* **15**, 986 (2022)
4. S. Lee, D. Kim, The Evaluation of Cross-Plane/in-Plane Thermal Diffusivity Using Laser Flash Apparatus. *Thermochim Acta* **653**, 126 (2017)
5. V. Kishore, N.S. Saxena, V.K. Saraswat, R. Sharma, K. Sharma, T.P. Sharma, Temperature Dependence of Effective Thermal Conductivity and Effective Thermal Diffusivity of CdZnSe Composite. *J Phys D Appl Phys* **39**, 2592 (2006)
6. L. Rivière, A. Lonjon, E. Dantras, C. Lacabanne, P. Olivier, N.R. Gleizes, Silver Fillers Aspect Ratio Influence on Electrical and Thermal Conductivity in PEEK/Ag Nanocomposites. *Eur Polym J* **85**, 115 (2016)
7. K.H. Lim, S.K. Kim, M.K. Chung, Improvement of the Thermal Diffusivity Measurement of Thin Samples by the Flash Method. *Thermochim Acta* **494**, 71 (2009)
8. G. Kalogiannakis, D. Van Hemelrijck, S. Longuemart, J. Ravi, A. Okasha, C. Glorieux, Thermal Characterization of Anisotropic Media in Photothermal Point, Line, and Grating Configuration. *J Appl Phys* **100**, 1 (2006)
9. S. Genna, N. Ucciardello, A Thermographic Technique for In-Plane Thermal Diffusivity Measurement of Electroplated Coatings. *Opt Laser Technol* **113**, 338 (2019)
10. T. Ishizaki, H. Nagano, Measurement of 3D Thermal Diffusivity Distribution with Lock-in Thermography and Application for High Thermal Conductivity CFRPs. *Infrared Phys Technol* **99**, 248 (2019)
11. W.N. Dos Santos, J.A. De Sousa, R. Gregorio, Thermal Conductivity Behaviour of Polymers around Glass Transition and Crystalline Melting Temperatures. *Polym Test* **32**, 987 (2013)
12. Z. Ran, Y. Yan, J. Li, Z. Qi, L. Yang, Determination of Thermal Expansion Coefficients for Unidirectional Fiber-Reinforced Composites. *Chin. J. Aeronaut.* **27**, 1180 (2014)
13. C. Dong, K. Li, Y. Jiang, D. Arola, D. Zhang, Evaluation of Thermal Expansion Coefficient of Carbon Fiber Reinforced Composites Using Electronic Speckle Interferometry. *Opt Express* **26**, 531 (2018)
14. R.D. Sweeting, X.L. Liu, Measurement of Thermal Conductivity for Fibre-Reinforced Composites. *Compos Part A Appl Sci Manuf* **35**, 933 (2004)

Publisher's Note

Springer Nature remains neutral with regard to jurisdictional claims in published maps and institutional affiliations.

Submit your manuscript to a SpringerOpen[®] journal and benefit from:

- Convenient online submission
- Rigorous peer review
- Open access: articles freely available online
- High visibility within the field
- Retaining the copyright to your article

Submit your next manuscript at ► [springeropen.com](https://www.springeropen.com)
